IJE TRANSACTIONS C: Aspects Vol. 36 No. 09, (September 2023) 1695-1703

International Journal of Engineering

Journal Homepage: www.ije.ir

Effect of nGO on Morphology, Mechanical Properties and Thermal Behavior of PLA/nGO Sheets Before and After Thermoforming: An Experimental Study

S. Honarmandnia[a,b], H. Shahrajabian*[a,b]

[a] *Department of Mechanical Engineering, Najafabad branch, Islamic Azad University, Najafabad, Iran*
[b] *Modern Manufacturing Technologies Research Center, Najafabad Branch, Islamic Azad University, Najafabad, Iran*

PAPER INFO

Paper history:
Received 01 July 2023
Received in revised form 23 July 2023
Accepted 25 July 2023

Keywords:
Poly Lactic Acid
Graphene Oxide Nanoparticles
Thermoforming Process
Tensile Test
Thickness Distribution
Differential Scanning Calorimetry Thermal Test

ABSTRACT

Today, contrary to the benefits and advantages that the use of polymer materials has had for humans, the use of these materials has caused environmental problems for human life due to their non-degradability in nature. Therefore, the use of biodegradable polymers such as polylactic acid (PLA) is increasing. One of the main applications of plastic materials is the production of disposable containers. In this research, the thermoforming process of PLA sheets reinforced with graphene oxide nanoparticles (nGO) (0.4 and 1 wt.%) was investigated. Scanning electron microscopy (SEM) and X-ray diffraction (XRD) were used to study the morphology of the samples before and after thermoforming. The mechanical properties before and after the thermoforming process were investigated by tensile test. The results showed that after the thermoforming process, the tensile strength of the sheets significantly increased, so that for the sample containing 1wt.% of nGO, the tensile strength increased by about 70%. The results of the thickness distribution investigation showed that the lowest amount of thickness reduction, approximately 68%, is related to the sample containing 1 wt. % of nGO. The results of the DSC thermal test showed that the degree of crystallinity of the samples significantly decreased after thermoforming.

***doi**: 10.5829/ije.2023.36.09c.14*

NOMENCLATURE

χ_c	Degree of crystallinity	ΔH_m^c	The heat of diffusion
ΔH_m	The melting enthalpy		

1. INTRODUCTION

Plastics based on petroleum materials such as polypropylene, polyethylene, polystyrene, and polyethylene terephthalate are strong, easy to process, durable, and relatively cheap. However, due to non-biodegradability, it creates problems when sending these materials to the waste stream. Biodegradable polymers have the potential to be a solution to the problem of plastic waste along with decreasing availability of landfills, global warming caused by increasing amounts of carbon dioxide in the atmosphere, and efforts to find sustainable or renewable raw materials. One of the most widely used biodegradable plastics is polylactic acid (PLA) [1]. Polylactic acid is a popular biodegradable and biocompatible polyester obtained from the condensation of lactic acid extracted from renewable sources such as corn, sugarcane, and sugar beet pomace [2]. Recent advances in the polymerization industry of PLA, which have led to a reduction in the price of this polymer material, have made PLA able to compete with oil-based industrial polymers in terms of price [3]. Although this polymer has advantages such as environmental compatibility, high strength, and modulus, and a cost comparable to petroleum-based polymers, its inherent fragility, low hydrophilicity, and gas permeability limit its use. Adding nano fillers in low content such as nano-clay [4, 5], cellulose nanofiber /Ag [6], carbon nanotube

*Corresponding Author Institutional Email: h.shahrajabian@pmc.iaun.ac.ir (H. Shahrajabian)

Please cite this article as: S. Honarmandnia, H. Shahrajabian, Effect of nGO on Morphology, Mechanical Properties and Thermal Behavior of PLA/nGO Sheets Before and After Thermoforming: An Experimental Study, ***International Journal of Engineering, Transactions C: Aspects***, Vol. 36, No. 09, (2023), 1695-1703

[7], silica [8], silicon carbide [9], and titanium oxide [10] increases the mechanical, thermal, electrical and antibacterial properties of the polymer matrix.

Recent researches have been shown that nano graphene oxide (nGO) is a suitable alternative for nano-clay in polymer matrix due to low density, high thermal conductivity, and high mechanical properties [11-14]. One of the attractive features of nGO is good interaction and combability with polymer matrices due to the polar structures of GO (containing carbonyls, hydroxyls, and epoxides groups) [15]. Sharifiana and Shahrajabian [16] increased the elastic modulus and strength of the PLA matrix by 32% and 18%, respectively, by incorporating nGO in content of 0.4 wt.%. Fredi et al. [17] improved strain at the break point of PLA from 5.3% to 10.0% by adding nGO in content of 0.25 phr. Khammassi et al. [18] added GO and Ag nanoparticles into the PLA matrix and observed that the crystallization temperature increased from 105.8℃ to 122.54℃, and the indentation load (in the nanoindentation test) enhanced by 28%.

Thermoforming is the most common method for producing disposable polymer containers [19]. Various polymer products, from electronic devices to medical products with materials of HDPE, ABS, PP, PS, and PLA, are produced by thermoforming method [20, 21]. In this process, a thermoplastic film or sheet which heated up to softening point of polymer (above glass transition temperature and lower melting point) is stretched into a female or male die by vacuum (vacuum assisted) or punch force (plug assisted) [22-24]. Various studies were done to investigate variables of the thermoforming process, such as viscoelastic behavior of sheet polymer, vacuum pressure, sheet temperature, heating time, and plug rate on product quality by experiments or finite element simulation [25-28]. They concluded that there are many independent variables which influence each other, and it is difficult to highlight an effective parameter.

PLA, due to its biodegradability, is a favorite polymer in packing industries [29], and therefore some research focused on thermoforming of PLA [30, 31]. Although a lot of research has been conducted on PLA thermoforming, little research has been done on the thermoforming process of PLA reinforced by nanofillers. Barletta and Puopolo [32] added calcium carbonate nanoparticles into PLA/PBS matrix, and studied the processability of the nanocomposite sheets by a thermoforming process. Considering the little research done on the thermoforming process of PLA nanocomposites, this research tries to investigate the thermoforming process of PLA nanocomposite sheets. The effect of nGO content on the thickness distribution of the sheets after forming was investigated. The influence of nGO on the morphology, mechanical properties, and thermal behavior of the sheet before and after thermoforming was examined.

2. MATERIALS AND METHODS

2. 1. Materials polylactic acid (PLA) granules (Bio-flex®F 6510 grade) of melting point 160℃, with a molecular weight of 198000 g/mol, a density of 1.3 g/cm^3 procured from Fkur GmbH, Germany. nGO in thickness of 3.2-4.5 μm was used as reinforcement in PLA matrix, and prepared from NANOSANY Co., Iran. Chloroform was used as the solvent of PLA, and obtained from Merck (Darmstadt, Germany).

2. 2. Preparation PLA and nGO were dried in a vacuum oven at 90℃ for 10h before processing. The nanocomposite films were prepared by a solvent casting technique. PLA granules weighing 5 g were dissolved on 110 ml of chloroform and mixed by a magnetic mixer for 5h to solve PLA granules completely. In the next step, nGO with a certain amount was dispersed in 15 ml of acetone solvent by ultrasonic homogenizer for 15 min. Then, nGO solution was added into PLA solution and stirred for 15 min by an ultrasonic homogenizer. Finally, the solution was poured into a glass container and was kept at ambient temperature for 24h to remove solvent and dry the sheets. To remove the solvent completely, the sheets were placed in a vacuum oven at 45℃ for 4 days. The composition of the prepared samples are stated in Table 1.

2. 3. Thermoforming All steps of the process, consisting of sheet preparation and thermoforming process, are presented in Figure 1. After preparing the nanocomposite sheets, the thermoforming process was done. The thermoforming was done by vacuum-assisted thermoforming technique. The product dimensions are shown in Figure 2. The polymer sheets were heated by a heater, which was placed on top of the sheets and followed by a vacuum process. A vacuum is applied when the temperature of the sheets reaches about 110℃. The temperature of the sheets was measured by a thermometer. Figure 3 shows thermoformed sheets.

2. 4. Characterization The morphology and structures of the PLA and PLA/nGO sheets were investigated by field emission scanning electron microscopy (FE-SEM) and X-ray diffraction (XRD). X-ray diffraction pattern was obtained by a PHILIPS 1050 with Cu-κα lines. Scanning was between 10° to 30° (2θ) by

TABLE 1. The composition of the samples

Sample	nGO (wt.%)	PLA (wt.%)
PLA	-	100
PLG0.4	0.4	99.6
PLG1	1	99

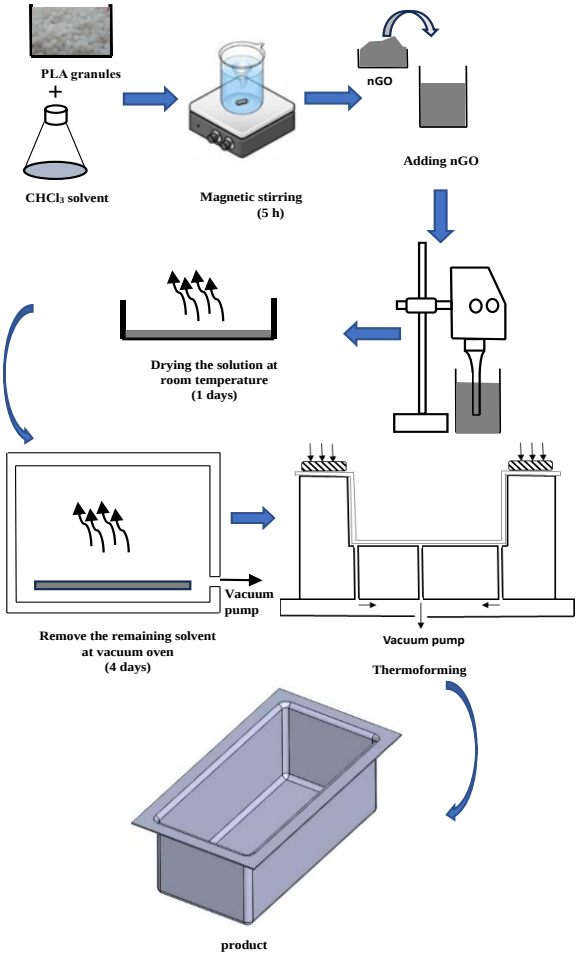

Figure 1. Schematic view of the process

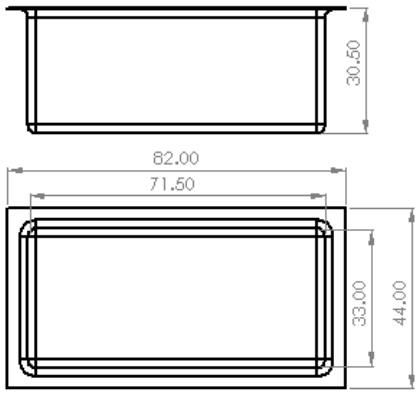

Figure 2. Product dimensions

step of 0.05° and scanning rate of 0.5/min. The mechanical properties of the unformed sheets and formed sheets were evaluated by tensile test. Tensile test was done at room temperature by HOUNFFIELD machine test model of H25KS at a feed rate of 1 mm/min according to ASTM D638 to measure tensile strength and elastic modulus

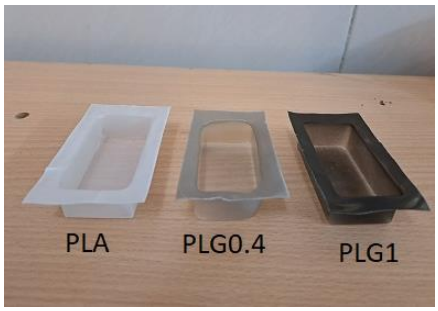

Figure 3. Thermoformed sheets

(Figure 4). The thermal behavior of the PLA and nanocomposite sheets was studied by differential scanning calorimetry (DSC) test. A SANAF DSC analyzer (Iran) in a temperature range of 20 ℃ to 210 ℃ by a heating rate of 10 ℃/min was used to determine the melting point (T_m), glass transition temperature (T_g), and melting enthalpy. The thickness variation (distribution) of the formed sheet was measured along cross-section on halved samples by a dial caliper with a resolution of 0.01 mm. The measurements were done in 8 points in the cut section. Figure 5 shows a schematic view of the section in which thickness variations were measured.

3. RESULTS

3. 1. Morphology Figure 4 shows the dispersion of nGO through the PLA matrix in the sample containing 1

(a)

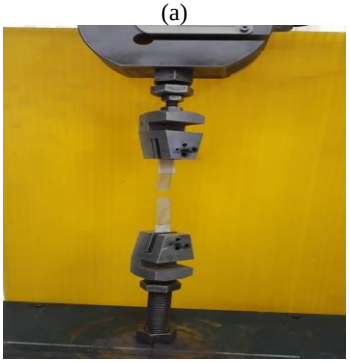

(b)

Figure 4. Tensile test set-up

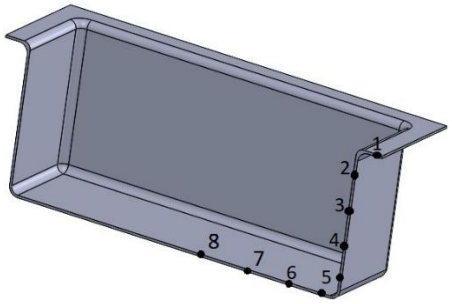

Figure 5. Points of thickness measurement

wt.% of nGO in two different magnifications by FE-SEM. As shown in Figure 4(a), GO nanoparticles have been dispersed in polymer matrix uniformly. Figure 4(b) shows the dispersion in higher magnification. In this figure, the uniform dispersion of nGO particles is more clearly visible, so that a nGO nanoparticle with an approximate length of 2 μm can be clearly seen in this figure. With a closer look, it can be seen the good adhesion of the nanoparticle to the polymer matrix. As shown in Figure 6, the nanoparticles the particles are well distributed on a nanoscale.

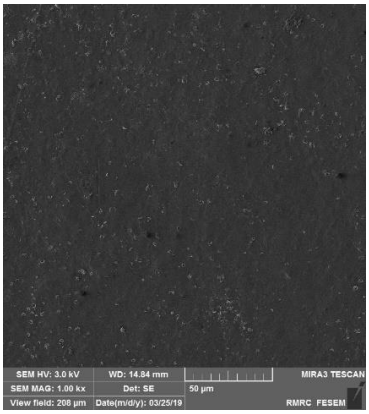

(a) CNF distribution in PLG1

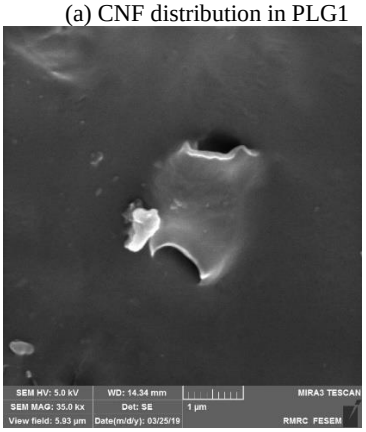

(b) GO nanoparticle in PLG1

Figure 6. FE-SEM images of the samples

3. 2. X-ray Diffraction The X-ray diffraction pattern of PLA and nanocomposite sheets before the thermoforming process is shown in Figure 7. A broad peak can be seen between 2θ=10˚to 2θ= 30˚for neat PLA sheet. This broad peak indicates the amorphous nature of the PLA crystal structure or has small crystals. The solution casting method can be the reason for the amorphous crystal structure, while PLA is a semi-crystalline polymer when it is produced by melting method. In the samples of PLG0.4 and PLG1, two peaks in 2θ=16.7˚and 2θ=19.3˚are observed. These two peaks represent planes of (200/110) and (203) in α type PLA with orthorhombic crystal structure, respectively. The presence of these two peaks in samples PLG0.4 and PLG1 indicates that adding nGO has caused the formation of the crystalline structure or an increase in the PLA crystalline percentage. GO nanoparticles have been able to act as nucleation sites for crystal formation and increase the crystalline rate of the PLA matrix. By observing the figure more closely, it can be seen that the peak intensity is higher for the samples of PLG0.4 and PLG1; as a result, the crystallization rate in this sample can be higher. The X-ray diffraction pattern of PLA and nanocomposite sheets after thermoforming process is shown in Figure 8. After the thermal forming process, the peaks at 16.7˚and 19.3˚have disappeared, and a new small peak has formed at 21.5˚, which corresponds to the (015) plane. The disappearance of the peaks after the thermoforming process shows that the severe deformation caused by the thermal forming process destroyed most of the crystals and changed other parts. By comparing Figures 7 and 8, it can be found that the application of severe thermal deformation can reduce the crystallization of the PLA matrix.

3. 3. Thickness distribution PLA and nanocomposite sheets were produced in the form of cubic

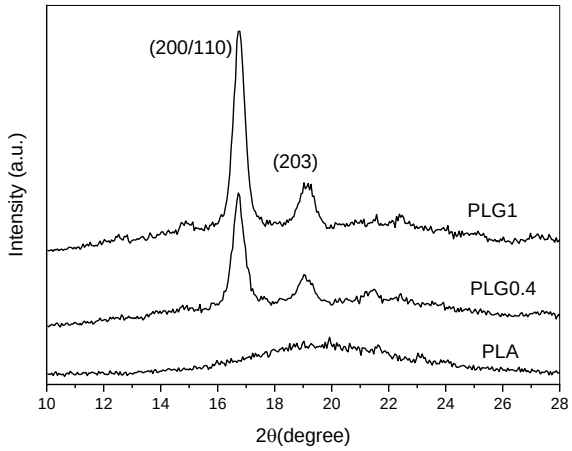

Figure 7. X-ray pattern of the sheets before thermoforming

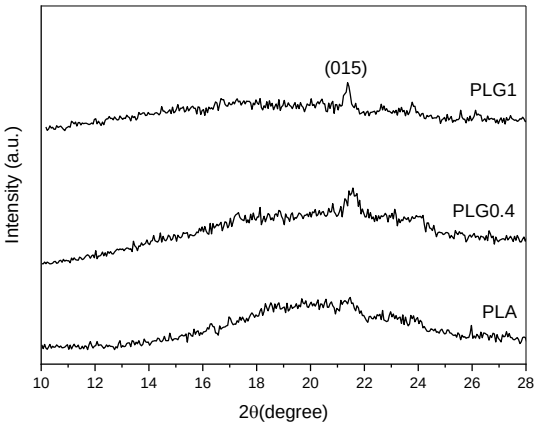

Figure 8. X-ray pattern of the sheets after thermoforming

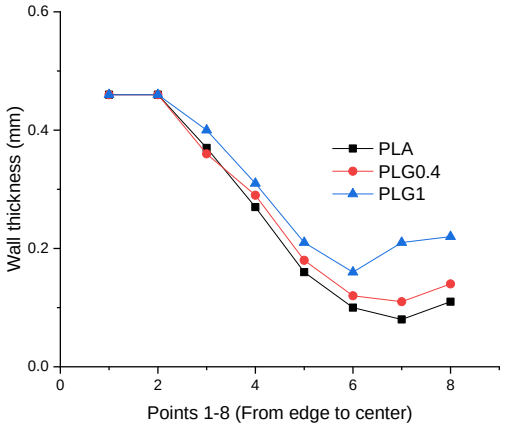

Figure 9. Thickness distribution of the samples

containers after thermoforming in female die. After the thermal forming process, the containers were cut, and the thickness of the sheets was measured at several points. The thickness distribution results for three samples of neat PLA, PLG0.4, and PLG1, are shown in Figure 9. As shown in this figure, the thickness of the edges of the sheets that have not been subjected to tension is almost equal to the thickness of the produced sheets (approximately 0.5 mm). By moving away from the edge and in the wall section of the containers, the thickness has decreased due to the tension. The decrease in thickness is increased by increasing the height from the edge of the container. On the side of the bottom of the container, this decrease in thickness continued until approaching the center of the bottom of the container; due to less tension, the thickness of the wall slightly increased. By comparing the samples, it can be observed that the reduction in wall thickness was lower for the samples containing graphene oxide nanoparticles. By increasing the percentage of graphene oxide nanoparticles from 0.4 to 1 wt.%, the thickness reduction is less. The maximum thickness reduction for neat PLA is 80%, while for PLG0.4 sample is 76%, and for PLG1 sample is 68%. This reduction in thickness changes for samples containing graphene oxide nanoparticles can be due to the higher strength of nanocomposite sheets because of the higher percentage of polylactic acid crystallization and the presence of graphene oxide nanoparticles.

3. 4. Mechanical Properties The mechanical properties of the sheets before and after thermoforming were evaluated by tensile test, and the stress-strain curves of the sheets before and after thermoforming are shown in Figures 10 and 11, respectively. The obtained data from stress-strain curves containing tensile strength, tensile modulus, and strain at break point (elongation) are presented in Tables 2 and 3. By adding graphene nano-oxide up to 1 wt.%, the elastic modulus increased from2630 MPa to 3670 MPa, which shows an increase in

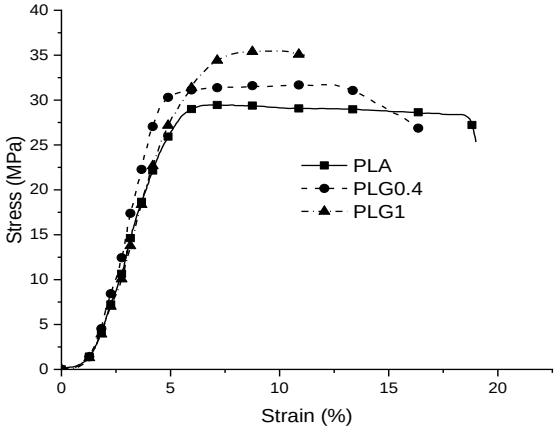

Figure 10. Stress-strain curve of the sheets before thermoforming

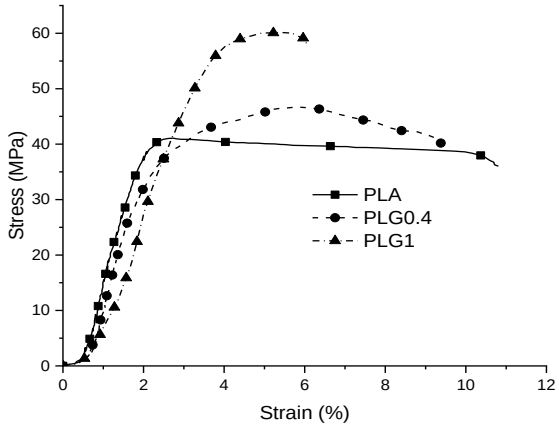

Figure 11. Stress-strain curve of the sheets after thermoforming

about 40%. The tensile strength also increased continuously from 28 MPa to 37 MPa by addition of graphene oxide nanoparticles up to 1 wt.%, which shows

TABLE 2. Obtained data from stress-strain curve of the samples before thermoforming

Sample	Young's modulus (MPa)	Tensile strength (MPa)	Elongation (%)
PLA	2630±130	28±3	21±1.5
PLG0.4	3452±170	32±4.5	17±1.25
PLG1	3670±150	37±6	12±2

TABLE 3. Obtained data from stress-strain curve of the samples after thermoforming

Sample	Young's modulus (MPa)	Tensile strength (MPa)	Elongation (%)
PLA	5210±160	42±4.5	11.5±1.85
PLG0.4	5310±150	46±6.5	10.2±1.65
PLG1	5430±170	63±8	6.8±1.42

a 32% increase in tensile strength. Unlike the elastic modulus and tensile strength, adding nGO into PLA has reduced the strain at the break point. The elongation for PLA is 21%, and by adding 1 wt.% of nGO, it has decreased to 12%. The results showed that adding nanoparticles has a significant positive effect on strength and elastic modulus. The reason for that can be considered to be an increase in the crystallinity of the PLA matrix, and the other is that the nanoparticles were able to support a part of the applied stress to the polymer matrix. After the sheets were subjected to thermoforming process and produced as plastic containers, tensile test samples were prepared from the bottom of the containers and subjected to tensile test to compare the mechanical properties of polymer and nanocomposite sheets before and after the thermoforming process to be compared, to determine the effect of the stretching process during thermoforming on the mechanical properties of the samples. Figure 11 shows the stress-strain curve of the samples after thermoforming. According to this curve, the elastic modulus of all three samples is almost the same and is about 5.3 GPa. By comparing this modulus with the elastic modulus of the samples before thermoforming process, it can be seen that the elastic modulus has significantly increased, so that for neat PLA, the modulus increased from 2630 MPa to 5210 MPa, which shows an increase of about 100%. The tensile strength for neat PLA is 42 MPa, and for the sample containing 1 wt.% of nGO increased to 63 MPa. By comparing the tensile strength of the samples before and after the thermoforming process, it can be understood that the strength had also increased significantly, so that for the sample containing 1 wt.% nGO, the tensile strength from 37 MPa before the thermoforming increased up to 63 MPa after thermoforming, which shows an increase of about 70%. The values of strain at the break point for all three samples after thermoforming show a significant decrease in compared to before thermoforming. Almost for all three samples, the strain has decreased by about 50%. From the tensile test results, it can be concluded that the strength and rigidity of polymer sheets after the thermoforming process increased and their flexibility decreased.

3. 5. Thermal Properties In order to investigate the thermal behavior and degree of crystallinity of PLA and nanocomposite sheets, a DSC test was performed. The melting scan for the sheets before the thermoforming process and after the thermoforming process are shown in Figures 12 and 13, respectively. Data related to DSC diagram, including glass transition temperature (Tg), melting temperature (Tm), heat of diffusion (ΔHm), and crystallinity (χ) for the sheets before and after the thermoforming process, is given in Tables 4 and 5, respectively. The degree of crystallinity can be expressed by the following formula (1):

$$X_c(\%) = \frac{\Delta H_m}{\Delta H_m^c} \times 100 \quad (1)$$

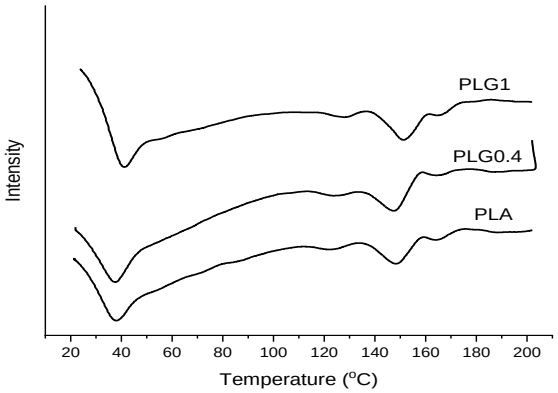

Figure 12. DSC melting scans of the sheets before thermoforming

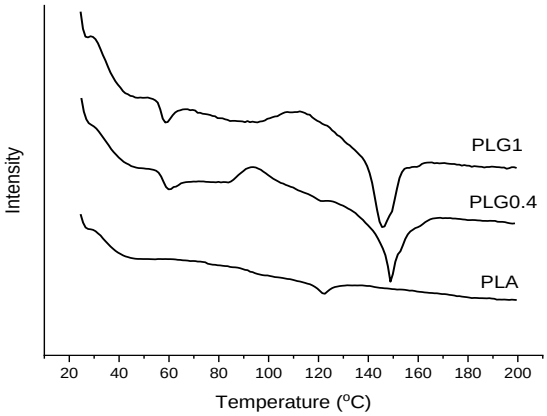

Figure 13. DSC melting scans of the sheets after thermoforming

TABLE 4. The DSC data of the sheets before thermoforming

Sample	T_g (°C)	T_m (°C)	ΔH_m (Jg^{-1})	χ (%)
PLA	37.7	147.8	5.4	5.7
PCNF	37.5	146.9	10.31	11.4
PCNFAg1	41.8	151.5	12.35	13.2

TABLE 5. The DSC data of the sheets after thermoforming

Sample	T_g (°C)	T_m (°C)	ΔH_m (Jg^{-1})	χ (%)
PLA	45	122.3	3.3	3.5
PCNF	60.2	149	6.05	6.5
PCNFAg1	59.2	146.7	8.52	10.98

where ΔH_m^c with value of 93 J/g is the heat of diffusion for 100% crystallite PLA.

Based on the data in Table 4, by adding nGO up to 1 wt.% to PLA, Tg has increased from 37.7℃ to 41.8℃. An increase in Tg showed that the presence of nGO reduced the mobility of polymer chains and prevented them from moving. Melting temperature data showed that the melting temperature has increased from 147.8℃ to 151.5℃. This increase in the melting point is due to an increase in the crystallinity and thickness of the lamellae. According to the crystallinity data obtained from the DSC scan, the degree of crystallinity in PLA has increased from 5.7 to 13.2% by adding nGO up to 1 wt.%. Crystallization results are also confirmed by x-ray test.

The DSC curve of the samples after thermoforming is given in Figure 13. By looking at this curve, it can be seen that the melting peak has become very small for neat PLA, which shows that the structure of this sheet has almost become amorphous after thermoforming. By comparing the data in Tables 4 and 5, it can be concluded that after the thermoforming process, Tg has significantly increased. For neat PLA, this temperature increased from 37.7℃ to 45℃, and for the PLG0.4 sample, it increased from 37.5 to 60.2, which is a significant increase. This increase in Tg is caused by the stretching of the polymer chains and their entanglement, which limits their mobility. The comparison of melting temperature data for samples containing nGO shows that the melting temperature before and after thermoforming has not changed significantly. But for neat PLA, it can be seen that the melting temperature decreased from 147.8℃ to 122.3℃, which shows a significant decrease. This is due to a considerable reduction in the crystallinity of the neat PLA. The data on the degree of crystallinity of the samples before and after thermoforming showed that the crystallinity has decreased for all samples.

4. CONCLUSION

In this research, thermoforming process of PLA/nGO nanocomposite sheets carried out. The x-ray diffraction patterns after thermoforming showed that the peacks in 16.7˚ and 19.3˚ disappeared, and a new small peak is formed at 21.5˚, which corresponds to the plane (015). According to the results of the thickness distribution of the samples after thermoforming, the decrease in wall thickness was lower for the samples containing graphene oxide nanoparticles. After thermoforming process, tensile strength of the samples significantly increased, so that for the sample containing 1 wt.% of nGO, the tensile strength increased from 37 MPa before the thermoforming to 63 MPa after the thermoforming process. By comparing the DSC thermal test data before and after thermoforming, it can be understood that the T_g has significantly increased after the thermal forming process. For neat PLA, this temperature increased from 37.7℃ to 45℃, and for the PLG0.4, it increased from 37.5℃ to 60.2℃. For all samples, the degree crystallinity decreased.

5. REFERENCES

1. Raquez, J.-M., Habibi, Y., Murariu, M. and Dubois, P., "Polylactide (pla)-based nanocomposites", ***Progress in Polymer Science***, Vol. 38, No. 10-11, (2013), 1504-1542. https://doi.org/10.1016/j.progpolymsci.2013.05.014
2. Armentano, I., Dottori, M., Fortunati, E., Mattioli, S. and Kenny, J., "Biodegradable polymer matrix nanocomposites for tissue engineering: A review", ***Polymer Degradation and Stability***, Vol. 95, No. 11, (2010), 2126-2146. https://doi.org/10.1016/j.polymdegradstab.2010.06.007
3. Liu, H. and Zhang, J., "Research progress in toughening modification of poly (lactic acid)", ***Journal of Polymer Science Part B: Polymer Physics***, Vol. 49, No. 15, (2011), 1051-1083. https://doi.org/10.1002/polb.22283
4. Stloukal, P., Pekařová, S., Kalendova, A., Mattausch, H., Laske, S., Holzer, C., Chitu, L., Bodner, S., Maier, G. and Slouf, M., "Kinetics and mechanism of the biodegradation of pla/clay nanocomposites during thermophilic phase of composting process", ***Waste Management***, Vol. 42, (2015), 31-40. https://doi.org/10.1016/j.wasman.2015.04. 006
5. Jadidi, H., Shahrajabian, H. and Moghri, M., "Using the mass method to produce pvc/clay nanocomposite foams: The effect of nano-clay and foaming conditions on density and cell size", ***Journal of Inorganic and Organometallic Polymers and Materials***, Vol. 26, (2016), 881-888. https://doi.org/10.1007/s10904-016-0386-7
6. Sheikh, K. and Shahrajabian, H., "Experimental study on mechanical, thermal and antibacterial properties of hybrid nanocomposites of pla/cnf/ag", ***International Journal of Engineering, Transactions B: Applications***, Vol. 34, No. 2, (2021), 500-507. doi: 10.5829/IJE.2021.34.02B.23.
7. Nian, L., Wang, M., Sun, X., Zeng, Y., Xie, Y., Cheng, S. and Cao, C., "Biodegradable active packaging: Components, preparation, and applications in the preservation of postharvest perishable fruits and vegetables", ***Critical Reviews in Food Science and Nutrition***, (2022), 1-36. https://doi.org/10.1080/10408398.2022.2122924
8. Vishal, K., Rajkumar, K., Sabarinathan, P. and Dhinakaran, V., "Mechanical and wear characteristics investigation on 3d printed silicon filled poly (lactic acid) biopolymer composite fabricated by fused deposition modeling", ***Silicon***, Vol. 14, No. 15, (2022), 9379-9391. https://doi.org/10.1007/s12633-022-01712-9

9. Stukhlyak, P., Buketov, A., Panin, S., Maruschak, P., Moroz, K., Poltaranin, M., Vukherer, T., Kornienko, L. and Lyukshin, B., "Structural fracture scales in shock-loaded epoxy composites", ***Physical Mesomechanics***, Vol. 18, (2015), 58-74. https://doi.org/10.1134/S1029959915010075

10. Mosalman, S., Rashahmadi, S. and Hasanzadeh, R., "The effect of tio2 nanoparticles on mechanical properties of poly methyl methacrylate nanocomposites (research note)", ***International Journal of Engineering, Transactions B: Applications***, Vol. 30, No. 5, (2017), 807-813. doi: 10.5829/idosi.ije.2017.30.05b.22.

11. Mohammadnia, M., Derakhshani, E. and Naghizadeh, A., "Defluoridation of aqueous solution by graphene and graphene oxide nanoparticles: Thermodynamic and isotherm studies", ***Iranian Journal of Chemistry and Chemical Engineering***, Vol. 39, No. 1, (2020), 67-77. doi: 10.30492/IJCCE.2020.33341.

12. Keshavarz, M.R. and Hassanajili, S., "Effect of graphene oxide reduction with l-ascorbic acid on electrical conductivity and mechanical properties of graphene oxide-epoxy nanocomposites", ***Iranian Journal of Chemistry and Chemical Engineering***, Vol. 40, No. 3, (2021), 731-742. doi: 10.30492/IJCCE.2020.38254.

13. Liu, L., Zhang, J., Zhao, J. and Liu, F., "Mechanical properties of graphene oxides", ***Nanoscale***, Vol. 4, No. 19, (2012), 5910-5916. https://doi.org/10.1039/C2NR31164J

14. Moslehi Niasar, M., Molaei, M. and Aghaei, A., "Electromagnetic wave absorption properties of barium ferrite/reduced graphene oxide nanocomposites", ***International Journal of Engineering, Transactions C: Aspects***, Vol. 34, No. 6, (2021), 1503-1511. doi: 10.5829/IJE.2021.34.06C.14.

15. Gao, W., "The chemistry of graphene oxide", ***Graphene oxide: Reduction Recipes, Spectroscopy, and Applications***, Vol., No., (2015), 61-95. https://doi.org/10.1007/978-3-319-15500-5_3

16. Sharifiana, M. and Shahrajabian, H., "The study of mechanical, thermal, and antibacterial properties of pla/graphene oxide/tio2 hybrid nanocomposites", ***Iranian Journal of Chemistry and Chemical Engineering***, Vol. 41, No. 3, (2022), 799-807. doi: 10.30492/IJCCE.2021.128785.4173.

17. Fredi, G., Karimi Jafari, M., Dorigato, A., Bikiaris, D.N. and Pegoretti, A., "Improving the thermomechanical properties of poly (lactic acid) via reduced graphene oxide and bioderived poly (decamethylene 2, 5-furandicarboxylate)", ***Materials***, Vol. 15, No. 4, (2022), 1316. https://doi.org/10.3390/ma15041316

18. Khammassi, S., Tarfaoui, M., Škrlová, K., Měřínská, D., Plachá, D. and Erchiqui, F., "Poly (lactic acid)(pla)-based nanocomposites: Impact of vermiculite, silver, and graphene oxide on thermal stability, isothermal crystallization, and local mechanical behavior", ***Journal of Composites Science***, Vol. 6, No. 4, (2022), 112. https://doi.org/10.3390/jcs6040112

19. Banús, N., Boada, I., Xiberta, P., Toldrà, P. and Bustins, N., "Deep learning for the quality control of thermoforming food packages", ***Scientific Reports***, Vol. 11, No. 1, (2021), 21887. https://doi.org/10.1038/s41598-021-01254-x

20. Ghorbani, S. and Matochi, A., "Thermoforming and its applications, a review", ***Basparesh***, Vol. 10, No. 2, (2020), 37-47. doi: 10.22063/BASPARESH.2020.2539.1483.

21. Choi, J., Han, C., Cho, S., Kim, K., Ahn, J., Del Orbe, D., Cho, I., Zhao, Z.-J., Oh, Y.S. and Hong, H., "Customizable, conformal, and stretchable 3d electronics via predistorted pattern generation and thermoforming", ***Science Advances***, Vol. 7, No. 42, (2021), eabj0694. doi: 10.1126/sciadv.abj0694.

22. Wittmann, L.-M. and Drummer, D., "Multilayer sheets for thermoforming non thermoformable polymers", ***Journal of Plastic Film & Sheeting***, Vol. 38, No. 2, (2022), 225-244. https://doi.org/10.1177/87560879211037387

23. Albilali, A.T., Baras, B.H. and Aldosari, M.A., "Evaluation of mechanical properties of different thermoplastic orthodontic retainer materials after thermoforming and thermocycling", ***Polymers***, Vol. 15, No. 7, (2023), 1610. https://doi.org/10.3390/polym15071610

24. Atmani, O., Abbès, F., Li, Y., Batkam, S. and Abbès, B., "Experimental and numerical investigation of the effects of sheet material, plug-assist tool material, and process conditions on the mechanical pre-stretching stage of plug-assist thermoforming", ***The International Journal of Advanced Manufacturing Technology***, Vol. 122, No. 7-8, (2022), 3217-3234. https://doi.org/10.1007/s00170-022-10125-2

25. Wei, H., "Optimisation on thermoforming of biodegradable poly (lactic acid)(pla) by numerical modelling", ***Polymers***, Vol. 13, No. 4, (2021), 654. https://doi.org/10.3390/polym13040654

26. O'Connor, C., Menary, G., Martin, P. and McConville, E., "Finite element analysis of the thermoforming of polypropylene", ***International Journal of Material Forming***, Vol. 1, No. Suppl 1, (2008), 779-782. https://doi.org/10.1007/s12289-008-0291-x

27. Ghobadnam, M., Mosaddegh, P., Rezaei Rejani, M., Amirabadi, H. and Ghaei, A., "Numerical and experimental analysis of hips sheets in thermoforming process", ***The International Journal of Advanced Manufacturing Technology***, Vol. 76, (2015), 1079-1089. https://doi.org/10.1007/s00170-014-6329-y

28. Turan, E., Konuşkan, Y., Yıldırım, N., Tuncalp, D., Inan, M., Yasin, O., Turan, B. and Kerimoğlu, V., "Digital twin modelling for optimizing the material consumption: A case study on sustainability improvement of thermoforming process", ***Sustainable Computing: Informatics and Systems***, Vol. 35, (2022), 100655. https://doi.org/10.1016/j.suscom.2022.100655

29. Gonon, H., Srisa, A., Promhuad, K., Chonhenchob, V., Bumbudsanpharoke, N., Jarupan, L. and Harnkarnsujarit, N., "Pla thermoformed trays incorporated with cinnamaldehyde and carvacrol as active biodegradable bakery packaging", ***Food Packaging and Shelf Life***, Vol. 38, (2023), 101123. https://doi.org/10.1016/j.fpsl.2023.101123

30. Sorimpuk, N., Choong, W. and Chua, B., "Design of thermoformable three dimensional-printed pla cast for fractured wrist", in IOP Conference Series: Materials Science and Engineering, IOP Publishing. Vol. 1217, (2022), 012002.

31. Swetha, T.A., Bora, A., Mohanrasu, K., Balaji, P., Raja, R., Ponnuchamy, K., Muthusamy, G. and Arun, A., "A comprehensive review on polylactic acid (pla)–synthesis, processing and application in food packaging", ***International Journal of Biological Macromolecules***, (2023), 123715. https://doi.org/10.1016/j.ijbiomac.2023.123715

32. Barletta, M. and Puopolo, M., "Thermoforming of compostable pla/pbs blends reinforced with highly hygroscopic calcium carbonate", ***Journal of Manufacturing Processes***, Vol. 56, (2020), 1185-1192. https://doi.org/10.1016/j.jmapro.2020.06.008

Persian Abstract

چکیده

امروزه درمقابل مزایایی که استفاده از مواد پلیمری برای انسان دارند، استفاده از این مواد به دلیل عدم سازگاری با محیط زیست باعث مشکلاتی برای محیط زیست شده است. بنابراین استفاده از پلیمرهای زیست تخریب پذیر مانند پلی لاکتیک اسید (PLA) رو به افزایش است. یکی از کاربردهای مهم مواد پلاستیکی برای تولید ظروف یکبار مصرف است. در این تحقیق فرآیند شکل دهی حرارتی ورق PLA تقویت شده با نانوذرات اکسید گرافن (nGO) به مقدار ۰/٤ و ۱ درصد وزنی بررسی شد. از میکروسکوپ الکترونی روبشی و تفرق اشعه ایکس برای مطالعه مورفولوژی نمونه‌ها قبل و بعد از شکل دهی حرارتی استفاده شد. خواص مکانیکی نمونه ها توسط آزمون کشش بررسی شد. نتایج آزمون کشش نشان داد که بعد از شکل دهی حرارتی استحکام کششی نمونه‌ها افزایش قابل توجهی می‌یابد، بطوریکه استحکام کششی نمونه حاوی ۱٪ وزنی nGO حدود ۷۰٪ افزایش یافت. نتایج توزیع ضخامت نشان داد کمترین میزان کاهش ضخامت به میزان ٦۸٪ مربوط به نمونه حاوی ۱٪ وزنی نانوذرات اکسید گرافن است. براساس نتایج آزمون حرارتی DSC، میزان تبلور همه نمونه‌ها پس از شکل دهی حرارتی کاهش می‌یابد.